



## Antimalarial ceramicines Q–T from *Chisocheton ceramicus*

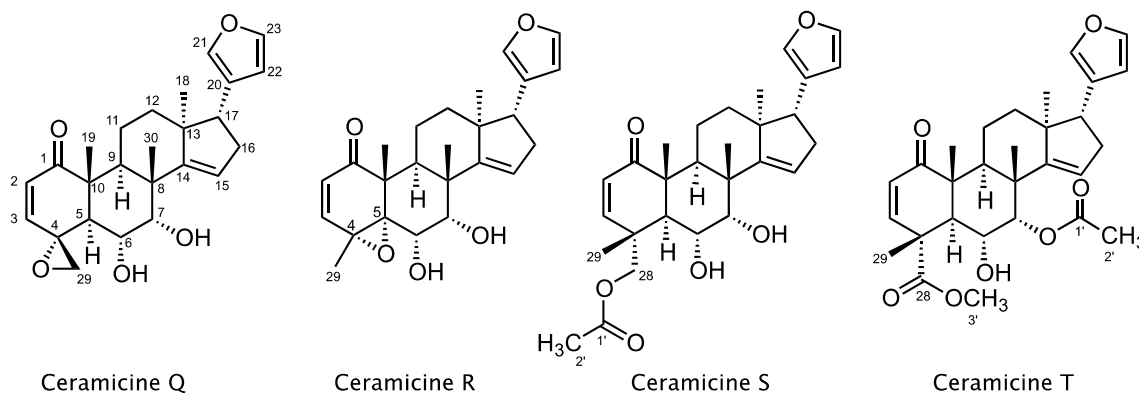
Alfarius Eko Nugroho<sup>1</sup> · Chin Piow Wong<sup>1</sup> · Yusuke Hirasawa<sup>1</sup> · Toshio Kaneda<sup>1</sup> · Takahiro Tougan<sup>2</sup> · Toshihiro Horii<sup>3</sup> · A. Hamid A. Hadi<sup>4</sup> · Hiroshi Morita<sup>1</sup>

Received: 9 March 2023 / Accepted: 29 April 2023 / Published online: 10 May 2023  
© The Author(s) under exclusive licence to The Japanese Society of Pharmacognosy 2023

### Abstract

Ceramicines are a series of limonoids that were isolated from the bark of Malaysian *Chisocheton ceramicus* (Meliaceae) and were known to show various biological activity. Four new limonoids, ceramicines Q–T (**1–4**) were isolated from the barks of *C. ceramicus*, and their structures were determined on the basis of the 1D and 2D NMR analyses in combination with calculated <sup>13</sup>C chemical shift data. Ceramicines Q–T (**1–4**) were established to be new limonoids with a cyclopentanone[α]phenanthren ring system with a β-furyl ring at C-17, and without a tetrahydrofuran ring like ceramicine B, which is characteristic of known ceramicines. Ceramicine R (**2**) exhibited potent antimalarial activity against *Plasmodium falciparum* 3D7 strain with IC<sub>50</sub> value of 2.8 μM.

### Graphical abstract



**Keywords** Ceramicines Q–T · Limonoids · *Chisocheton ceramicus* · Meliaceae · Antimalarial activity

✉ Yusuke Hirasawa  
y-hirasawa@hoshi.ac.jp

✉ Hiroshi Morita  
moritah@hoshi.ac.jp

<sup>1</sup> Faculty of Pharmaceutical Sciences, Hoshi University, Ebara 2-4-41 Shinagawa-ku, Tokyo 142-8501, Japan

<sup>2</sup> Department of Cellular Immunology, Research Institute for Microbial Diseases, Osaka University, 3-1 Yamadaoka, Suita, Osaka 565-0871, Japan

<sup>3</sup> Department of Malaria Vaccine Development, Research Institute for Microbial Diseases, Osaka University, 3-1 Yamadaoka, Suita, Osaka 565-0871, Japan

<sup>4</sup> Department of Chemistry, Faculty of Science, University of Malaya, 50603 Kuala Lumpur, Malaysia

### Introduction

The plants belonging to Meliaceae have been reported to produce limonoids [1]. In our search for new bioactive compounds from medicinal plants, we have reported the isolation of new limonoids from plants of this genus [2–15], and alkaloids [16–23] and coumarins [24] showing antimalarial activity or inhibiting acetylcholinesterase. Ceramicine B, in particular, has been reported to show a strong lipid droplets accumulation (LDA) inhibitory activity on mouse pre-adipocyte cell line (MC3T3-G2/PA6) [6–8] and also anti-melanin deposition activity [9]. With the purpose of

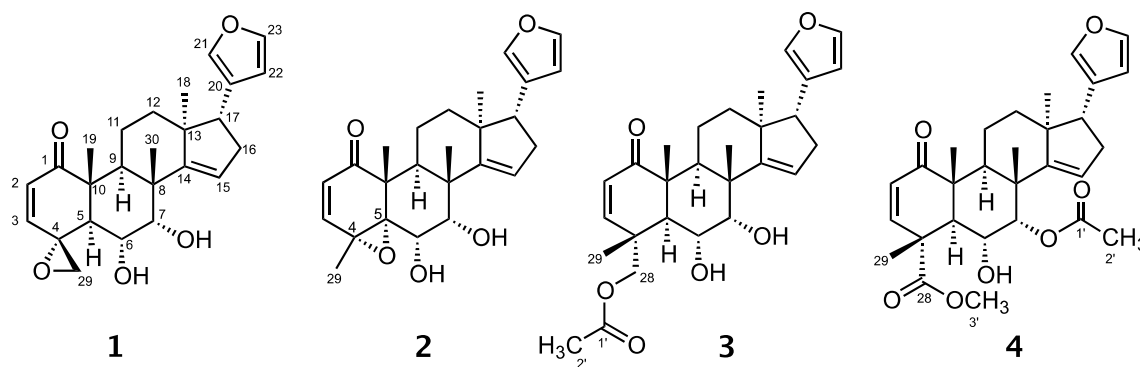


**Fig. 1** Structures of **1–4**

**Table 1**  $^1\text{H}$  and  $^{13}\text{C}$  NMR data of **1** and **2** in  $\text{CDCl}_3$

No.	<b>1</b>		<b>2</b>	
	$\delta_{\text{H}}(J, \text{Hz})$	$\delta_{\text{C}}$	$\delta_{\text{H}}(J, \text{Hz})$	$\delta_{\text{C}}$
1		202.0		199.5
2	5.98 (1H, d, 10.2)	131.0	5.94 (1H, d, 10.0)	129.9
3	6.23 (1H, d, 10.2)	146.7	6.70 (1H, d, 10.0)	148.2
4		60.4		55.6
5	3.01 (1H, d, 10.8)	43.5		68.0 <sup>a</sup>
6	4.12 (1H, dd, 10.8, 2.4)	66.7	4.50 (1H, m)	63.8
7	3.92 (1H, d, 2.4)	74.3	4.12 (1H, brd, 2.7)	77.7
8		43.3		43.6
9	2.69 (1H, dd, 11.8, 5.8)	32.5	2.85 (1H, m)	29.7
10		50.3		50.3
11a	1.56 (1H, m)	17.8	1.61 (1H, m)	18.5
11b	2.51 (1H, m)		2.47 (1H, m)	
12a	1.63 (1H, m)	33.2	1.61 (1H, m)	32.6
12b	1.93 (1H, m)		1.94 (1H, m)	
13		47.0		47.2
14		159.6		160.0 <sup>a</sup>
15	5.54 (1H, brd, 2.0)	119.6	5.60 (1H, brd, 2.0)	119.9
16a	2.39 (1H, ddd, 15.2, 7.3, 3.4)	34.4	2.42 (1H, ddd, 15.4, 7.2, 3.4)	34.3
16b	2.56 (1H, dd, 15.2, 11.5)		2.57 (1H, dd, 15.4, 11.0)	
17	2.85 (1H, dd, 11.5, 7.3)	62.0	2.88 (1H, m)	52.1
18	0.92 (3H, s)	21.5	0.94 (3H, s)	21.2
19	1.31 (3H, s)	14.8	1.32 (3H, s)	19.2
20		124.6		124.4
21	7.25 (1H, brs)	139.7	7.26 (1H, m)	139.7
22	6.30 (1H, brs)	111.1	6.29 (1H, brs)	111.0
23	7.37 (1H, brt, 1.8)	142.5	7.39 (1H, brt, 1.6)	142.7
29a	3.09 (1H, d, 3.5)	60.4	1.86 (1H, s)	18.4
29b	3.65 (1H, d, 3.6)			
30	1.17 (3H, s)	26.2	1.29 (3H, s)	25.8

<sup>a</sup>Based on HMBC correlations

discovering limonoids with biological activity, we further investigated the constituents of *C. ceramicus* which led to

the isolation of four new limonoids, ceramicines Q–T (**1–4**), and ceramicine R (**2**) showed potent antimalarial activity

**Table 2**  $^1\text{H}$  and  $^{13}\text{C}$  NMR data of **3** and **4** in  $\text{CDCl}_3$ 

No.	<b>3</b>		<b>4</b>	
	$\delta_{\text{H}}(J, \text{Hz})$	$\delta_{\text{C}}$	$\delta_{\text{H}}(J, \text{Hz})$	$\delta_{\text{C}}$
1		204.7		203.2
2	5.80 (1H, d, 10.2)	126.0	5.86 (1H, d, 10.1)	126.9
3	6.27 (1H, m)	151.3	6.32 (1H, d, 10.1)	146.4
4		40.9		47.7
5	2.38 (1H, d, 11.2)	41.7	3.27 (1H, d, 11.8)	44.0
6	4.20 (1H, brd, 11.2)	67.9	4.23 (1H, m)	66.5
7	3.94 (1H, brd, 2.2)	76.0	5.35 (1H, brd, 2.2)	78.5
8		44.0		42.8
9	2.47 (1H, m)	33.1	2.57 (1H, dd, 11.5, 4.9)	35.3
10		49.2		48.3
11a	1.52 (1H, m)	17.6	1.57 (1H, m)	18.5
11b	2.47 (1H, m)		2.47 (1H, m)	
12a	1.57 (1H, m)	32.8	1.66 (1H, m)	33.7
12b	1.90 (1H, m)		1.94 (1H, m)	
13		47.1		47.0
14		161.0		158.4
15	5.55 (1H, brd, 2.2)	119.8	5.43 (1H, m)	120.0
16a	2.42 (1H, m)	34.3	2.34 (1H, m)	34.3
16b	2.53 (1H, m)		2.39 (1H, m)	
17	2.85 (1H, dd, 10.8, 7.4)	51.9	2.83 (1H, dd, 10.5, 7.7)	52.0
18	0.90 (3H, s)	21.3	0.89 (3H, s)	22.2
19	1.32 (3H, s)	17.0	1.30 (3H, s)	16.3
20		124.4		124.7
21	7.25 (1H, brs)	139.7	7.24 (1H, brs)	139.7
22	6.28 (1H, m)	111.0	6.29 (1H, brs)	111.0
23	7.38 (1H, brs)	142.6	7.38 (1H, brt, 1.5)	142.6
28a	4.03 (1H, d, 10.8)	72.0		175.8
28b	4.59 (1H, d, 10.8)			
29a	1.36 (3H, s)	17.0	1.61 (3H, s)	17.0
29b				
30	1.19 (3H, s)	26.6	1.26 (3H, s)	26.7
1'		171.3		171.8
2'	2.01 (3H, s)	21.0	2.04 (3H, s)	21.0
3'			3.65 (3H, s)	52.7

(Fig. 1). Their structures were determined on the basis of NMR and MS spectroscopic analyses in combination with NMR chemical shifts calculations.

## Results and discussions

Compounds **1–4** were obtained as optically active white amorphous solids. The  $^1\text{H}$  and  $^{13}\text{C}$  NMR data (Tables 1 and 2) suggested the identity of **1–4** as ceramicine derivatives.

Ceramicine Q (**1**) was obtained as an optically active,  $[\alpha]_{\text{D}}^{27} + 119$  ( $c$  1.0,  $\text{CHCl}_3$ ), white amorphous solid and was

revealed to have the molecular formula  $\text{C}_{25}\text{H}_{30}\text{O}_5$ , by HRESITOFMS [ $m/z$  433.1991 ( $\text{M} + \text{Na}$ ) $^+$ ,  $\Delta - 1.4$  mmu]. IR absorptions implied the presence of  $\alpha,\beta$ -unsaturated ketone ( $1683\text{ cm}^{-1}$ ) and hydroxy ( $3461\text{ cm}^{-1}$ ) groups.  $^1\text{H}$  and  $^{13}\text{C}$  NMR data (Table 1) revealed 25 carbon resonances due to one carbonyl, two  $\text{sp}^2$  quaternary carbons, four  $\text{sp}^3$  quaternary carbons, six  $\text{sp}^2$  methines, five  $\text{sp}^3$  methines, four  $\text{sp}^3$  methylenes, and three methyls. Among them, four  $\text{sp}^3$  carbons ( $\delta_{\text{C}}$  60.4, 60.4, 66.7, and 74.3) and two  $\text{sp}^2$  methines ( $\delta_{\text{C}}$  139.7 and 142.5) were ascribed to those bearing an oxygen atom.

Analyses of the HSQC and  $^1\text{H}$ - $^1\text{H}$  COSY spectra (Fig. 2) revealed the presence of four partial structures; **a** (C-2 and C-3), **b** (C-5~C-7), **c** (C-9, C-11, and C-12), **d** (C-15~C-17), and **e** (C-22~C-23). HMBC correlations of  $\text{H}_3$ -18 to C-12, C-13, C-14 and C-17 suggested the connectivity of **c**, **d**, and C-14 through C-13. HMBC correlations of H-17 to C-21, H-16 to C-20, and H-23 to C-20 and C-21 suggested the presence of  $\beta$ -furyl at C-17, and the correlation of  $\text{H}_2$ -16 to C-13 and C-14 completed the structure of ring D. The presence of ring C was deduced from the HMBC cross-peaks of  $\text{H}_3$ -30 to C-7, C-8, C-9 and C-14, and the connectivity of **b**, C-1, C-5, and C-19 through C-10 was suggested by the HMBC correlations of  $\text{H}_3$ -19 to C-1, C-5, C-9 and C-10. HMBC correlations of H-2 to C-10 and C-4, and H-3 to C-1 and C-5 suggested the presence of ring A. Finally, HMBC correlations of H-3 to C-29 ( $\delta_{\text{C}}$  60.4) suggested the presence of 1-oxaspiro[2.5]oct-4-ene of **1** as shown in Fig. 2.

The relative configuration of **1** was assigned by analyses of the  $^1\text{H}$ - $^1\text{H}$  coupling constant data and the NOESY correlations (Fig. 2). First, H-6, H-17,  $\text{CH}_3$ -19, and  $\text{CH}_3$ -30 were assigned to be  $\beta$ -axially oriented from the NOESY correlations of H-6/ $\text{H}_3$ -19 and  $\text{H}_3$ -30/H-17 and  $\text{H}_3$ -19, while H-5, H-9 and  $\text{CH}_3$ -18 were deduced to possess  $\alpha$ -orientation from the NOESY correlations of H-9/H-5 and  $\text{H}_3$ -18. Both H-6 and H-7 should possess  $\beta$ -orientation because of the multiplicity pattern of H-6 (dd, 10.8, 2.4) and H-7 (d, 2.4). The stereochemistry of epoxy ring was elucidated to be as shown in Fig. 2 by the presence of NOESY correlations of H-29a/H-3 and  $\text{H}_3$ -19, and H-29b/ $\text{H}_3$ -19.

Ceramicine R (**2**),  $[\alpha]_{\text{D}}^{28} 126$  ( $c$  0.5,  $\text{CHCl}_3$ ), was revealed to have the molecular formula  $\text{C}_{25}\text{H}_{30}\text{O}_5$  by HRESITOFMS. Its NMR data are highly similar to **1**. However, the signals for oxymethylene of  $\text{H}_2$ -29 in **1** are not observed in **2**, and a methyl signal ( $\delta_{\text{H}}$  1.86) and two  $\text{sp}^3$  quaternary carbons bearing an oxygen atom ( $\delta_{\text{C}}$  55.6 and 68.0) are observed instead. Analysis of the 2D NMR data including HMBC and NOESY (Fig. 3) correlations supported the structure of **2** to be 4,5-epoxy derivative as shown in Fig. 1. Specifically, the HMBC correlations of  $\text{H}_3$ -29 to C-3, C-4 ( $\delta_{\text{C}}$  55.6) and C-5 ( $\delta_{\text{C}}$  68.0), and  $\text{H}_3$ -19 to C-5 supported its functionality in the structure of **2**.

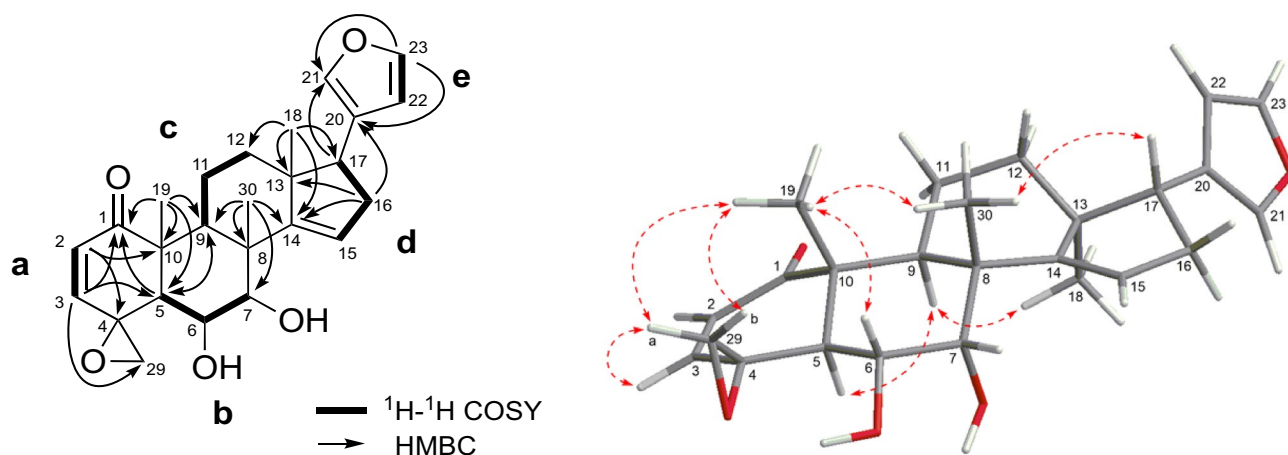


**Fig. 2** Selected 2D NMR correlations of **1**

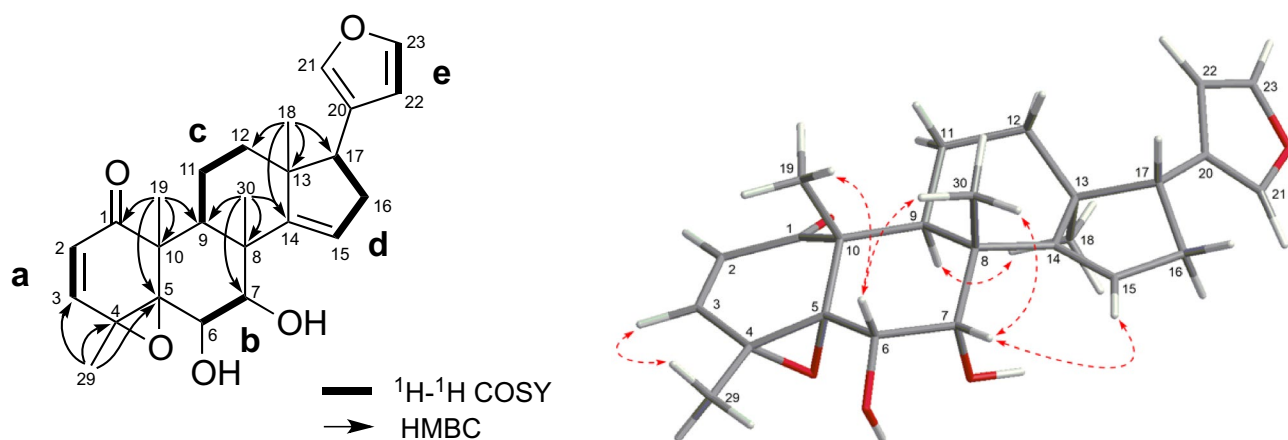


**Fig. 3** Selected 2D NMR correlations of **2**

NOESY correlations of H-6/H<sub>3</sub>-19 and H<sub>3</sub>-30, H-7/H<sub>3</sub>-30 and H-15, and H-9/H<sub>3</sub>-18 supported the stereochemistry of **2**. Configurations of H-6 and H-7 taking  $\beta$ -orientation like as in **1** also supported by proton  $^3J$  coupling constant ( $J=2.7$  Hz).

The remaining problem regarding stereochemistry is that of epoxy in positions 4 and 5. Only the presence of two NOESY correlations of H-3/H<sub>3</sub>-29 and H-6/H<sub>3</sub>-19 is difficult to determine unequivocally. Therefore, we compared the predicted NMR chemical shifts of the two possible diastereomers, **2a** (4,5- $\alpha$ -epoxy) and **2b** (4,5- $\beta$ -epoxy) as shown below (Fig. 4), calculated for the  $\omega$ B97X-V/6-311+G\* optimized conformations using  $\omega$ B97X-V/6-311+G\*(2df,2p).

Conformational searches and chemical shift calculations for compounds **2a** and **2b** were performed with the Spartan'20 software [25]. Stable conformers up to 40 kJ/mol for **2a** and **2b** were initially searched using the Merck molecular force field (MMFF) method. Stable conformers

suggested were optimized using Hartree–Fock (HF)/3-21G (40 kJ/mol) and  $\omega$ B97X-D/6-31G\* (15 kJ/mol). Final energy optimization for the Boltzmann distribution was conducted at the  $\omega$ B97X-V/6-311+G\*(2df,2p) level of theory. NMR properties were calculated at the  $\omega$ B97X-V/6-311+G\*(2df,2p) level of theory and scaled. The obtained chemical shifts were corrected using the Boltzmann distribution to give calculated  $^{13}\text{C}$  chemical shifts.

The  $^{13}\text{C}$  chemical shift differences of predicted and experimental data are shown as graph in Fig. 5. Two atoms of C-6 and C-9 in **2b** shows a deviation of greater than 5 ppm, but the average deviation is less than 2 ppm in **2a**. Overall, the  $^{13}\text{C}$  chemical shifts predicted for structure **2a** (Fig. 4) correlate very well with those observed for ceramicine R (**2**).

Thus, we propose that the correct structure of ceramicine R (**2**) is the structure **2a**. The prediction of  $^{13}\text{C}$  chemical shifts by DFT calculation is a very powerful tool for

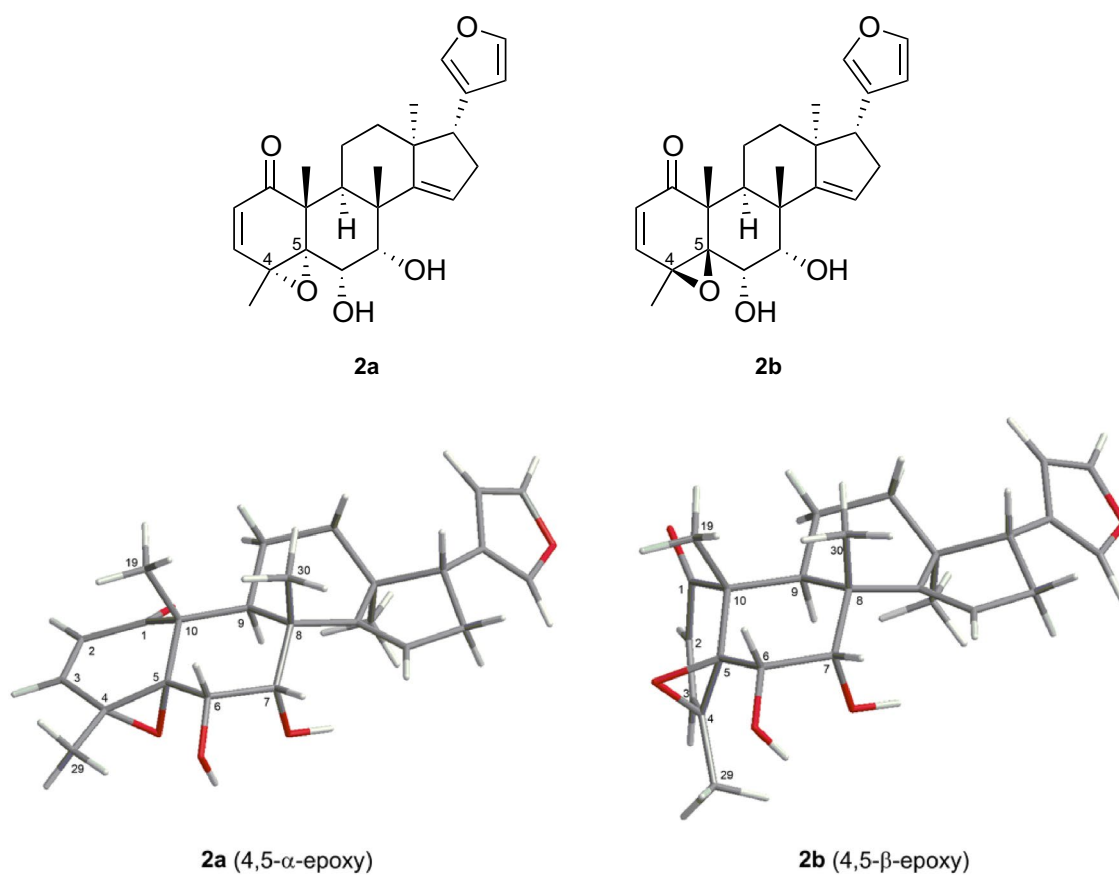


**Fig. 4** Structures of the lowest-energy conformation of the two possible isomers (**2a** and **2b**) of ceramicine R (**2**)

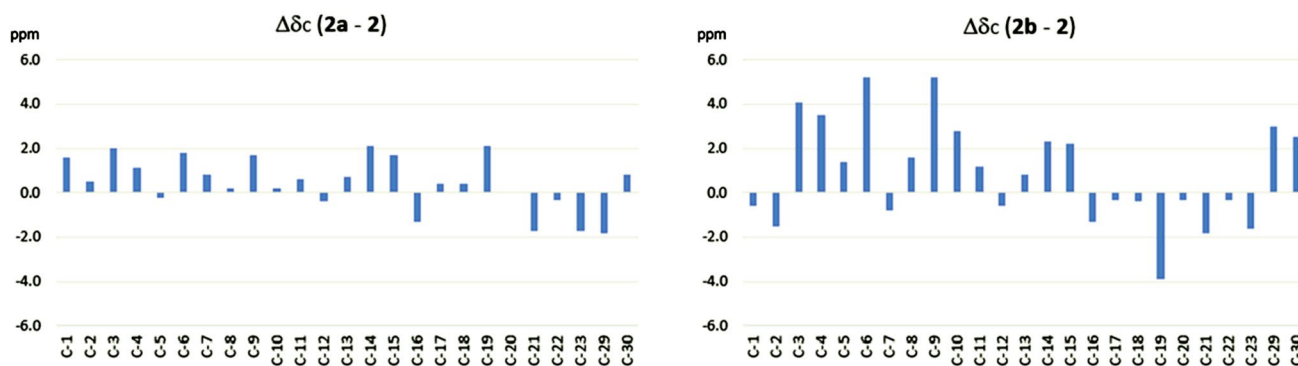


**Fig. 5** Parts per million difference between the calculated  $^{13}\text{C}$  NMR shifts for the two possible isomers (**2a** and **2b**) and the experimental data of ceramicine R (**2**)

screening proposed structures and should be used more widely.

Ceramicine S (**3**),  $[\alpha]_{\text{D}}^{27} + 34$  ( $c$  1.0,  $\text{CHCl}_3$ ), was revealed to have the molecular formula  $\text{C}_{28}\text{H}_{36}\text{O}_6$  by HRESITOFMS.

Its  $^1\text{H}$  and  $^{13}\text{C}$  NMR data are highly similar to ceramicine R (**2**) (Table 2). However, the NMR data of **3** suggested that the oxymethylene moiety [ $\delta_{\text{H}}$  4.03 (d, 10.8), 4.59 (d, 10.8);  $\delta_{\text{C}}$  72.0] with acetyl group [ $\delta_{\text{H}}$  2.01 (3H, s);  $\delta_{\text{C}}$  21.0 and

171.3] was observed instead of the epoxide function in **2**. IR absorptions implied the presence of  $\alpha,\beta$ -unsaturated ketone ( $1684\text{ cm}^{-1}$ ), hydroxy ( $3502\text{ cm}^{-1}$ ), and acetyl ( $1733\text{ cm}^{-1}$ ) groups. The HMBC correlations of  $\text{H}_2\text{-28}$  and  $\text{H}_3\text{-2}'$  to C-1' ( $\delta_{\text{C}} 171.3$ ) supported its functionality in the structure of **3**. Finally, the NOESY correlations confirmed the position of the oxymethylene moiety with the acetyl group at C-28 and the  $\alpha$  orientation of the hydroxy at C-6 and C-7 (See Supplementary Information).

By HRESITOFMS, ceramicine T (**4**),  $[\alpha]_{\text{D}}^{28} + 67$  ( $c$  0.5,  $\text{CHCl}_3$ ), was revealed to have the molecular formula  $\text{C}_{29}\text{H}_{36}\text{O}_7$ . Their NMR data are also highly similar to **3**, differing only on the signals assigned to the presence of one acetyl and one methoxy carbonyl groups in **4** and the disappearance of oxy-methylene protons of **3**. IR absorptions implied the presence of  $\alpha,\beta$ -unsaturated ketone ( $1683\text{ cm}^{-1}$ ), hydroxy ( $3534\text{ cm}^{-1}$ ), and acetyl and/or methoxycarbonyl ( $1732\text{ cm}^{-1}$ ) groups. Analysis of the NMR data revealed the presence of a cyclopentanone[ $\alpha$ ]phenanthren ring system with a  $\beta$ -furyl ring at C-17.

The planar structure of **4** was deduced from the  $^1\text{H}$ - $^1\text{H}$  COSY correlations and the especially HMBC correlations of  $\text{H}_3\text{-29}$  and  $\text{H}_3\text{-3}'$  to C-28 and  $\text{H}_3\text{-30}$  to C-7. The relative configuration of **4** was then deduced from the NOESY correlations of H-6/ $\text{H}_3\text{-19}$ ,  $\text{H}_3\text{-29}$  and  $\text{H}_3\text{-30}$ , H-9/H-5 and  $\text{H}_3\text{-18}$ , H-7/ $\text{H}_3\text{-30}$ , and H-12a/ $\text{H}_3\text{-30}$  and H-17 (See Supplementary Information). Thus, the structure of **4** was proposed to be as shown in Fig. 1.

Considering that **1**–**4** were isolated from the same extract as ceramicine B [3], their absolute configurations were assumed to be similar to ceramicine B based on the biogenetic relationships. Ceramicines Q and R might be generated from a cyclopentanone[ $\alpha$ ]phenanthren ring system followed by oxidative decarboxylation at C-28.

## Antimalarial activity

Ceramicines Q–T (**1**–**4**) were tested for antimalarial activity against *Plasmodium falciparum* 3D7 strain. The assay showed that **2** had potent in vitro antimalarial activity [the half-maximal (50%) inhibitory concentration ( $\text{IC}_{50}$ ) =  $2.8\text{ }\mu\text{M}$ , whereas **1**, **3**, and **4** did not ( $> 5.0\text{ }\mu\text{M}$ )].

Previously, we also reported some limonoids, ceramicines A–D with a cyclopentanone[ $\alpha$ ]phenanthren ring system with a tetrahydrofuran ring and a  $\beta$ -furyl ring from the barks of *C. ceramicus*, exhibited antimalarial activity against *P. falciparum* 3D7 in vitro [2, 3].

The activity might be depending on their unique cyclopentanone[ $\alpha$ ]phenanthren ring system and also be influenced by the presence of a tetrahydrofuran ring and its substituent patterns around rings A and B.

## Experimental section

### General experimental procedures

Optical rotations were measured on a JASCO DIP-1000 polarimeter. UV spectra were recorded on a Shimadzu UVmini-1240 spectrophotometer and IR spectra on a JASCO FT/IR-4100 spectrophotometer. High-resolution ESI MS were obtained on a JMS-T100LP (JEOL).  $^1\text{H}$  and 2D NMR spectra were measured on a 400 MHz or 600 MHz spectrometer at 300 K, while  $^{13}\text{C}$  NMR spectra were on a 100 MHz or 150 MHz spectrometer. The residual solvent peaks were used as internal standards ( $\delta_{\text{H}} 7.26$  and  $\delta_{\text{C}} 77.0$  for  $\text{CDCl}_3$ ,  $\delta_{\text{H}} 3.31$  and  $\delta_{\text{C}} 49.0$  for  $\text{CD}_3\text{OD}$ ).

### Material

The barks of *C. ceramicus* were collected in Terengganu, Malaysia in July 2013. The botanical identification was made by Prof. A. Hamid A. Hadi, University of Malaya. Voucher specimens (No. HOSHI13CCB) are deposited in the department of Pharmacognosy Hoshi University.

### Extraction and isolation

The barks of *C. ceramicus* (8 kg) were extracted with MeOH to obtain 1.43 kg of extract. The MeOH extract was successively partitioned with *n*-hexane, EtOAc, *n*-BuOH and water. The *n*-hexane-soluble materials were separated further by silica gel column chromatography (*n*-hexane/EtOAc 1:0→1:1,  $\text{CHCl}_3/\text{MeOH}$  1:0→0:1) to obtain 10 fractions (A–J). Fraction I was separated further with a ODS silica gel column ( $\text{MeOH}/\text{H}_2\text{O}$  7:3→1:0, acetone) to obtain 6 fractions (I-1–I-6). Fraction I-3 was also separated by HPLC (Shiseido ODS MGII  $30\times 250\text{ mm}$ , 85% aqueous MeOH at 8.0 mL/min, UV detection at 210 nm) into 7 fractions (I-3-a–I-3-g). Fraction I-3-c, I-3-d, and I-3-f are ceramicine F, G and B, respectively. Separation of fraction I-3-a by HPLC (Nacalai tesque Cholesterol  $10\times 250\text{ mm}$ , 65% aqueous MeCN at 2.0 mL/min, UV detection at 210 nm) yielded ceramicine Q (**1**) (6.0 mg, 0.000075%,  $t_{\text{R}}$  18.6 min) and ceramicine R (**2**) (0.8 mg, 0.00001%,  $t_{\text{R}}$  21.0 min).

Separation of fraction I-3-e by HPLC (Nacalai tesque Cholesterol  $10\times 250\text{ mm}$ , 60% aqueous MeCN at 2.0 mL/min, UV detection at 210 nm) yielded ceramicine S (**3**) (10.6 mg, 0.00013%,  $t_{\text{R}}$  44.0 min) and ceramicine T (**4**) (1.0 mg, 0.000012%,  $t_{\text{R}}$  50.0 min).

Ceramicine Q (**1**): white amorphous solid;  $[\alpha]_{\text{D}}^{27} + 119$  ( $c$  1.0,  $\text{CHCl}_3$ ); UV (MeOH)  $\lambda_{\text{max}}$  ( $\epsilon$ ) 204 (10,000) nm; CD (MeOH)  $\lambda_{\text{max}}$  ( $\Delta\epsilon$ ) 337 (– 1.59) and 216 (10.3) nm; IR (Zn-Se)  $\nu_{\text{max}}$  3461 and  $1683\text{ cm}^{-1}$ ;  $^1\text{H}$  and  $^{13}\text{C}$  NMR data (Table 1); ESIMS  $m/z$  433 ( $\text{M} + \text{Na}$ ) $^+$ ; HRESIMS  $m/z$



433.1977 (M + Na)<sup>+</sup> [calcd for C<sub>25</sub>H<sub>30</sub>O<sub>5</sub>Na (M + Na)<sup>+</sup>: 433.1991].

Ceramicine R (2): white amorphous solid;  $[\alpha]_D^{28} + 126$  (c 0.5, CHCl<sub>3</sub>); UV (MeOH)  $\lambda_{\max} (\epsilon)$  204 (10,700) nm; CD (MeOH)  $\lambda_{\max} (\Delta\epsilon)$  336 (− 2.36), 250 (2.18) and 230 (1.52) nm; IR (Zn-Se)  $\nu_{\max}$  3450 and 1697 cm<sup>−1</sup>; <sup>1</sup>H and <sup>13</sup>C NMR data (Table 1); ESIMS *m/z* 433 (M + Na)<sup>+</sup>; HRESIMS *m/z* 433.1982 (M + Na)<sup>+</sup> [calcd for C<sub>25</sub>H<sub>30</sub>O<sub>5</sub>Na (M + Na)<sup>+</sup>: 433.1991].

Ceramicine S (3): white amorphous solid;  $[\alpha]_D^{27} + 34$  (c 1.0, CHCl<sub>3</sub>); UV (MeOH)  $\lambda_{\max} (\epsilon)$  204 (11,900) nm; CD (MeOH)  $\lambda_{\max} (\Delta\epsilon)$  333 (− 2.96), 249 (Δ 0.36), 230 (Δ − 0.35) and 212 (Δ 3.79) nm; IR (Zn-Se)  $\nu_{\max}$  3502, 1733 and 1684 cm<sup>−1</sup>; <sup>1</sup>H and <sup>13</sup>C NMR data (Table 1); ESIMS *m/z* 491 (M + Na)<sup>+</sup>; HRESIMS *m/z* 491.2417 (M + Na)<sup>+</sup> [calcd for C<sub>28</sub>H<sub>36</sub>O<sub>6</sub>Na (M + Na)<sup>+</sup>: 491.2410].

Ceramicine T (4): white amorphous solid;  $[\alpha]_D^{28} + 67$  (c 0.5, CHCl<sub>3</sub>); UV (MeOH)  $\lambda_{\max} (\epsilon)$  204 (12,000) nm; CD (MeOH)  $\lambda_{\max} (\Delta\epsilon)$  336 (− 2.21), 234 (− 12.6), 206 (17.0) nm; IR (Zn-Se)  $\nu_{\max}$  3534, 1732 and 1683 cm<sup>−1</sup>; <sup>1</sup>H and <sup>13</sup>C NMR data (Table 2); ESIMS *m/z* 519 (M + Na)<sup>+</sup>; HRESIMS *m/z* 519.2361 (M + Na)<sup>+</sup> [calcd for C<sub>29</sub>H<sub>36</sub>O<sub>7</sub>Na (M + Na)<sup>+</sup>: 519.2359].

### <sup>13</sup>C chemical shift calculations

Conformational searches and chemical shift calculations for compounds **2a** and **2b** were performed with the Spartan'20 software [25]. Stable conformers up to 40 kJ/mol for **2a** and **2b** were initially searched using the Merck molecular force field (MMFF) method. Stable conformers suggested were optimized using Hartree–Fock (HF)/3-21G (40 kJ/mol) and ωB97X-D/6-31G\* (15 kJ/mol). Final energy optimization for the Boltzmann distribution was conducted at the ωB97X-V/6-311+G\*(2df,2p) level of theory. NMR properties were calculated at the ωB97X-V/6-311+G\*(2df,2p) level of theory and scaled. The obtained chemical shifts were corrected using the Boltzmann distribution to give calculated <sup>13</sup>C chemical shifts.

### Parasite strain culture

*P. falciparum* laboratory strain 3D7 was obtained from Prof. Masatsugu Kimura (Osaka City University, Osaka, Japan). For the assessment of antimalarial activity of the compounds in vitro, the parasites were cultured in Roswell Park Memorial Institute (RPMI) 1640 medium supplemented with 0.5 g/L L-glutamine, 5.96 g/L HEPES, 2 g/L sodium bicarbonate (NaHCO<sub>3</sub>), 50 mg/L hypoxanthine, 10 mg/L gentamicin, 10% heat-inactivated human serum, and red blood cells (RBCs) at a 3% hematocrit in an atmosphere of 5% CO<sub>2</sub>, 5% O<sub>2</sub>, and 90% N<sub>2</sub> at 37 °C as previously described

[26]. Ring-form parasites were collected using the sorbitol synchronization technique [27]. Briefly, the cultured parasites were collected by centrifugation at 840 g for 5 min at room temperature, suspended in a fivefold volume of 5% D-sorbitol (Nacalai Tesque, Kyoto, Japan) for 10 min at room temperature, and then they were washed twice with RPMI 1640 medium to remove the D-sorbitol. The utilization of blood samples of healthy Japanese volunteers for the parasite culture was approved by the institutional review committee of the Research Institute for Microbial Diseases (RIMD), Osaka University (approval number: 22-3).

### Antimalarial activity

Ring-form-synchronized parasites were cultured with compounds **1–4** at sequentially decreasing concentrations (50, 15, 5, 1.5, 0.5, and 0.15 μM) for 48 h for the flow cytometric analysis using an automated hematology analyzer, XN-30. The XN-30 analyzer was equipped with a prototype algorithm for cultured falciparum parasites [prototype; software version: 01-03, (build 16)] and used specific reagents (CELLPACK DCL, SULFOLYSER, Lysercell M, and Fluorocell M) (Sysmex, Kobe, Japan) [28, 29]. Approximately 100 μL of the culture suspension diluted with 100 μL phosphate-buffered saline was added to a BD Microtainer MAP Microtube for Automated Process K<sub>2</sub> EDTA 1.0 mg tube (Becton Dickinson and Co., Franklin Lakes, NJ, USA) and loaded onto the XN-30 analyzer with an auto-sampler as described in the instrument manual (Sysmex). The parasitemia (MI-RBC%) was automatically reported [25]. Then 0.5% DMSO alone or containing 5 μM artemisinin was used as the negative and positive controls, respectively. The growth inhibition (GI) rate was calculated from the MI-RBC% according to the following equation:

$$GI(\%) = 100 - \frac{(\text{test sample} - \text{positive control})}{(\text{negative control} - \text{positive control})} \times 100$$

The IC<sub>50</sub> was calculated from GI (%) using GraphPad Prism version 5.0 (GraphPad Prism Software, San Diego, CA, USA) [30].

**Supplementary Information** The online version contains supplementary material available at <https://doi.org/10.1007/s11418-023-01706-w>.

**Acknowledgements** We thank Prof. Masatsugu Kimura (Osaka City University, Osaka, Japan) for the kind gift of the 3D7 strain, Mr. Yuji Toya and Dr. Kinya Uchihashi (Sysmex) for the setting of the XN-30 analyzer and Ms. Toshie Ishisaka and Ms. Sawako Itagaki for their technical assistance. This work was partly supported by JSPS KAKENHI (JP 19K07152 and JP 22K06671 to MH) and (JP 16K08309 to AEN), Japan.

## References

- Zhang Y, Xu H (2017) Recent progress in the chemistry and biology of limonoids. *RSC Adv* 7:35191–35220
- Mohamad K, Hirasawa Y, Lim CS, Awang K, Hadi AHA, Takeya K, Morita H (2008) Ceramicine A and walsogyne A, novel limonoids from two species of Meliaceae. *Tetrahedron Lett* 49:4276–4278
- Mohamad K, Hirasawa Y, Litaudon M, Awang K, Hadi AHA, Takeya K, Ekasari W, Widyawaruyanti A, Zaini NC, Morita H (2009) Ceramicine B-D, a new antiplasmodial limonoids from *Chisocheton ceramicus*. *Bioorg Med Chem* 17:727–730
- Wong CP, Shimada M, Nagakura Y, Nugroho AE, Hirasawa Y, Kaneda T, Awang K, Hadi AHA, Mohamad K, Shiro M, Morita H (2011) Ceramicine E-I, new limonoids from *Chisocheton ceramicus*. *Chem Pharm Bull* 59:407–411
- Wong C, Shimada M, Nugroho AE, Hirasawa Y, Kaneda T, Hadi AHA, Osamu S, Morita H (2012) Ceramicines J-L, new limonoids from *Chisocheton ceramicus*. *J Nat Med* 66:566–570
- Nugroho AE, Hashimoto A, Wong C-P, Yokoe H, Tsubuki M, Kaneda T, Hadi AHA, Morita H (2018) Ceramicines M-P from *Chisocheton ceramicus*: isolation and structure–activity relationship study. *J Nat Med* 72:64–72
- Wong CP, Deguchi J, Nugroho AE, Kaneda T, Hadi AHA, Morita H (2013) Ceramicines from *Chisocheton ceramicus* as lipid-droplets accumulation inhibitors. *Bioorg Med Chem Lett* 23:1786–1788
- Wong CP, Kaneda T, Hadi AHA, Morita H (2014) Ceramicine B, a limonoid with anti-lipid droplets accumulation activity from *Chisocheton ceramicus*. *J Nat Med* 68:22–30
- Iijima C, Wong CP, Nugroho AE, Sotozono Y, Someya S, Hirasawa Y, Kaneda T, Hadi AHA, Morita H (2016) Anti-melanin deposition activity of ceramicines from *Chisocheton ceramicus*. *J Nat Med* 70:702–707
- Nugroho AE, Okuda M, Yamamoto Y, Hirasawa Y, Wong C-P, Kaneda T, Shirota O, Hadi AHA, Morita H (2013) Walsogyne B – G, limonoids from *Walsura chrysogyne*. *Tetrahedron* 69:4139–4145
- Nugroho AE, Nakajima S, Wong C-P, Hirasawa Y, Kaneda T, Shirota O, Tougan T, Horii T, Hadi AHA, Morita H (2022) Walsogyne H – O from *Walsura chrysogyne*. *J Nat Med* 76:94–101
- Prema WCP, Awouafack MD, Nugroho AE, Win YY, Win NN, Ngwe H, Morita H, Morita H (2019) Two new quassinoids and other constituents from the *Picrasma javanica* wood and their biological activities. *J Nat Med* 73:589–596
- Prema WCP, Kodama T, Nugroho AE, El-Desoky AH, Awouafack MD, Win YY, Ngwe H, Abe I, Morita H, Morita H (2020) Three new quassinoids isolated from the wood of *Picrasma javanica* and their anti-Vpr activities. *J Nat Med* 74:571–578
- Nugroho AE, Hirasawa Y, Kaneda T, Shirota O, Matsuno M, Mizukami H, Morita H (2021) Triterpenoids from *Walsura trichostemon*. *J Nat Med* 75:415–422
- Nugroho AE, Tange M, Kusakabe Y, Hirasawa Y, Kaneda T, Shirota O, Matsuno M, Mizukami H, Tougan T, Horii T, Morita H (2022) Triterpenoids from *Walsura trichostemon*. *J Nat Med* 76:756–764
- Nugroho AE, Zhang W, Hirasawa Y, Tang Y, Wong CP, Kaneda T, Hadi AHA, Morita H (2018) Bisleuconothines B-D, modified eburnane-aspidosperma bisindole alkaloids from *Leuconotis griffithii*. *J Nat Prod* 81:2600–2604
- Nugroho AE, Ono Y, Jin E, Hirasawa Y, Kaneda T, Rahman A, Kusumawati I, Tougan T, Horii T, Zaini NC, Morita H (2021) Bisindole alkaloids from *Voacanga grandifolia* leaves. *J Nat Med* 75:408–414
- Tang Y, Nugroho AE, Hirasawa Y, Tougan T, Horii T, Hamid A, Hadi A, Morita H (2019) Leucophyllinines A and B, bisindole alkaloids from *Leuconotis eugeniifolia*. *J Nat Med* 73:533–540
- Amelia P, Nugroho AE, Hirasawa Y, Kaneda T, Tougan T, Horii T, Morita H (2019) Indole alkaloids from *Tabernaemontana macrocarpa* Jack. *J Nat Med* 73:820–825
- Amelia P, Nugroho AE, Hirasawa Y, Kaneda T, Tougan T, Horii T, Morita H (2021) Two new bisindole alkaloids from *Tabernaemontana macrocarpa* Jack. *J Nat Med* 75:633–642
- Hirasawa Y, Yasuda R, Minami W, Hirata M, Nugroho AE, Tougan T, Uchiyama N, Hakamatsuka T, Horii T, Morita H (2021) Divaricamine A, a new anti-malarial trimeric monoterpenoid indole alkaloid from *Tabernaemontana divaricata*. *Tetrahedron Lett* 83:153423
- Hirasawa Y, Agawa-Kakimoto M, Zaima K, Uchiyama N, Goda Y, Morita H (2021) Complandine F, a novel dimeric alkaloid from *Lycopodium complanatum*. *J Nat Med* 75:403–407
- Hirasawa Y, Tanaka T, Hirasawa S, Wong CP, Uchiyama N, Kaneda T, Goda Y, Morita H (2022) Cliniatines A-C, new Amaryllidaceae alkaloids from *Clivia miniata*, inhibiting Acetylcholinesterase. *J Nat Med* 76:171–177
- Ogasawara A, Noguchi R, Shigi T, Nugroho AE, Hirasawa Y, Kaneda T, Tougan T, Horii T, Hamid A, Hadi A, Morita H (2022) Caloforines A-G, coumarines from the bark of *Calophyllum scribbitifolium*. *J Nat Med* 76:645–653
- Spartan'20 (2020) WaveFunction, Inc., Irvine, CA
- Trager W, Jensen JB (1976) Human malaria parasites in continuous culture. *Science* 193:673–675. <https://doi.org/10.1126/science.781840>
- Lambros C, Vanderberg JP (1979) Synchronization of *Plasmodium falciparum* erythrocytic stages in culture. *J Parasitol* 65:418–420
- Tougan T, Suzuki Y, Itagaki S, Izuka M, Toya Y, Uchihashi K, Horii T (2018) An automated haematology analyzer XN-30 distinguishes developmental stages of falciparum malaria parasite cultured in vitro. *Malar J* 17:59. <https://doi.org/10.1186/s12936-018-2208-6>
- Toya Y, Tougan T, Horii T, Uchihashi K (2021) Lysercell M enhances the detection of stage-specific Plasmodium-infected red blood cells in the automated hematology analyzer XN-31 prototype. *Parasitol Int* 80:102206. <https://doi.org/10.1016/j.parint.2020.102206>
- Tougan T, Toya Y, Uchihashi K, Horii T (2019) Application of the automated haematology analyzer XN-30 for discovery and development of anti-malarial drugs. *Malar J* 18:8. <https://doi.org/10.1186/s12936-019-2642-0>

**Publisher's Note** Springer Nature remains neutral with regard to jurisdictional claims in published maps and institutional affiliations.

Springer Nature or its licensor (e.g. a society or other partner) holds exclusive rights to this article under a publishing agreement with the author(s) or other rightsholder(s); author self-archiving of the accepted manuscript version of this article is solely governed by the terms of such publishing agreement and applicable law.